

# Protein oxidation and aggregation in UVA-irradiated *Escherichia coli* cells as signs of accelerated cellular senescence

Franziska Bosshard,<sup>1,2</sup> Kathrin Riedel,<sup>3</sup>  
Thomas Schneider,<sup>3</sup> Carina Geiser,<sup>1</sup>  
Margarete Bucheli<sup>1</sup> and Thomas Egli<sup>1,2\*</sup>

<sup>1</sup>Eawag, Swiss Federal Institute of Aquatic Science and Technology, P.O. Box 611, CH-8600 Dübendorf, Switzerland.

<sup>2</sup>Institute of Biogeochemistry and Pollutant Dynamics, ETH Zürich, CH-8092 Zürich, Switzerland.

<sup>3</sup>Institute of Plant Biology, University of Zürich, CH-8057 Zürich, Switzerland.

## Summary

Solar disinfection (SODIS) is a simple drinking water treatment method that improves microbiological water quality where other means are unavailable. It makes use of the deleterious effect of solar irradiation on pathogenic microbes and viruses. A positive impact on health has been documented in several epidemiological studies. However, the molecular mechanisms damaging cells during this simple treatment are not yet fully understood. Here we show that protein damage is crucial in the process of inactivation by sunlight. Protein damages in UVA-irradiated *Escherichia coli* cells have been evaluated by an immunoblot method for carbonylated proteins and an aggregation assay based on semi-quantitative proteomics. A wide spectrum of structural and enzymatic proteins within the cell is affected by carbonylation and aggregation. Vital cellular functions like the transcription and translation apparatus, transport systems, amino acid synthesis and degradation, respiration, ATP synthesis, glycolysis, the TCA cycle, chaperone functions and catalase are targeted by UVA irradiation. The protein damage pattern caused by SODIS strongly resembles the pattern caused by reactive oxygen stress. Hence, sunlight probably accelerates cellular senescence and leads to the inactivation and finally death of UVA-irradiated cells.

## Introduction

Sunlight is an important environmental factor that has influenced life since it appeared on earth. In many surface ecosystems microorganisms are transiently affected by sunlight; a prominent example are the surface waters of the sea (Jeffrey *et al.*, 2005). Bacterial enteric pathogens have the gut as their primary habitat and are therefore usually more sensitive to solar radiation than environmental strains that had the chance to adapt during evolution. The deleterious effect of solar radiation on enteric bacteria is used to improve microbiological drinking water quality by solar disinfection (SODIS), a simple drinking water treatment method (Wegelin *et al.*, 1994). A positive impact on health has been documented in several epidemiological studies, e.g. during a cholera epidemic in Kenya, where a reduction of diarrhoea cases among SODIS users of 88% was observed (Conroy *et al.*, 2001). SODIS was recently added to the WHO list of recommend drinking water treatment methods. Although the effectiveness of SODIS against enteric bacterial pathogens is well documented, the underlying cellular inactivation mechanisms are not yet well understood.

Protein oxidation is known to be a key factor in cellular ageing in eukaryotes (Grune *et al.*, 2004) and was recently also found to be important in bacteria (Nyström, 2006). The tertiary structure of oxidized proteins is thermodynamically instable and, therefore, oxidized proteins tend to expose hydrophobic amino acids to the outside, with the consequences of agglutination and cross-linking (Squier, 2001; Grune *et al.*, 2004; Chiti, 2006). The accumulation of protein aggregates is associated with age-related diseases and senescence in many different organisms (Mazzulli *et al.*, 2006), also in bacteria, where aggregation was suggested to lead to cell death (Maisonneuve *et al.*, 2008a). The accumulation of protein aggregates in a cell can either result from an increased level of damaged proteins or be due to a less efficient protein degradation and repair. In eukaryotic cells the proteasome is in charge of protein turnover and removal of oxidized proteins, and it might even itself be a target of oxidative stress (Friguet, 2006). Damaged proteins in aggregates are not easily accessible for proteases. Indeed, it was suggested that protein fragmentation and

Received 27 January, 2010; accepted 21 April, 2010. \*For correspondence. E-mail: egli@eawag.ch; Tel. (+41) 44 823 5158; Fax (+41) 44 823 5547.

cross-linking might make proteins resistant to proteolytic digestion (Gianazza *et al.*, 2007). In bacterial cells carbonylated proteins are predominantly found in protein aggregates where they seem to escape degradation (Maisonneuve *et al.*, 2008b).

Very early loss of energy-generating systems within the cytoplasmic membrane (respiration and ATPase activity) appear to be a primary cause for cellular die-off during sunlight irradiation (Bosshard *et al.*, 2009a). This loss of enzymatic functions suggests that protein damages at the cytoplasmic membrane are involved in cell inactivation during SODIS. The underlying cause for protein damage most probably is oxidative stress. For example, it was reported that reactive oxygen species (ROS) originate predominantly from 'leakage' in the respiratory chain (Yuanbin *et al.*, 2002) and, therefore, it is believed that respiratory chain enzymes are also the first targets of oxygen stress (Choksi *et al.*, 2008). This is also supported by the observation that adaptation to UVA light clearly induced many genes of the oxidative defence system (Berney *et al.*, 2007). There is much evidence that proteins are a very important target of oxidative damage within cells. Whereas lipid peroxidation and DNA modification for a long time was the most investigated radical-mediated process, more recent studies indicate also proteins as important targets of oxidative damage with severe consequences for cell functioning (Bourdon and Blache, 2001). Surprisingly, protein damage seems to be crucial in highly ionizing radiation-resistant bacteria such as *Deinococcus radiodurans* where the degree of resistance appears to be determined by the level of oxidative protein damage caused during irradiation. The authors are convinced that protein and not DNA is the principle target of the biological action in sensitive bacteria and that extreme resistance is based on protein protection, as suggested recently (Daly *et al.*, 2007). One protection mechanism in *D. radiodurans* is to reduce cytosolic iron ions up to three times and, instead, to increase manganese ions up to 300 times. By this, the cells are capable to reduce iron-dependent Fenton reactions causing protein oxidation and in this way to protect enzymatic functions. Another more common line of defence against oxidative damage found in many cell types, e.g. in *Escherichia coli*, are the enzymes catalase, superoxide dismutase and peroxidases (Gross, 2007; Fredrickson *et al.*, 2008).

Oxidized proteins are believed to severely impair cell viability (Berlett and Stadtman, 1997). The most widespread method to assess the level of oxidatively damaged proteins within a cell is by measuring the level of newly introduced carbonylation sites in proteins (Requena *et al.*, 2003). Detection by a Western blot assay is used after blotting of one- or two-dimensional (1D or 2D) gels (Levine, 2002). Several authors have

used this assay method successfully in microorganisms, after UVA treatment (Hoerter *et al.*, 2005a,b), with oxidative stress (Tamarit *et al.*, 1998; Cabisco *et al.*, 2000), and with senescence and ageing (Dukan and Nystrom, 1998). Carbonylation is a basic damage leading to covalent cross-linking of proteins and the formation of protein aggregates by several mechanisms (Stadtman and Levine, 2003). These covalently cross-linked protein aggregates are stable in SDS-PAGE because they withstand the reducing conditions (by DTT or mercaptoethanol) and are not affected by the detergent (SDS), a fact that was already utilized early to examine oxidation effects of hydroxyl radicals on several purified enzymes. An increase in protein size was interpreted as a sign of protein aggregation, a decrease as protein fragmentation (Davies, 1987; Davies and Delsignore, 1987). Other authors used advanced protein identification methods instead of gel electrophoresis to detect oxidatively cross-linked and fragmented proteins (Mirzaei and Regnier, 2007).

In this study, a proteome analysis of *E. coli* cells irradiated with UVA light in a reproducible laboratory setting is presented. It gives an indication of which proteins are damaged during SODIS and an insight into the underlying mechanisms leading to cell death during exposure to sunlight is obtained.

## Results

Protein damage during SODIS was characterized in this article with the help of several different methods. Carbonylation damages were detected already with very low fluences by a sensitive immunoblot method. These oxidative damages are prerequisites for protein aggregation, which we detected at higher fluences with gel electrophoresis. Tandem mass spectrometry in combination with a semi-quantitative spectral count analysis helped to identify proteins that tend to aggregate or fragment during SODIS. Furthermore, a massive loss of protein spots was observed on 2D gels, which brought us to test the possibility of leaking of the cells during SODIS. Dissolved organic carbon (DOC) analysis revealed that only a very small percentage of cellular C was leaking out during irradiation. Interestingly, in raw extracts of irradiated cells, mild centrifugation was able to separate a big part of the cellular proteins as insoluble protein aggregates.

### *Qualitative aggregation effect on whole cell proteome assessed by gel electrophoresis*

One surprising effect of UVA irradiation was that cellular proteins became unable to properly separate with traditional gel electrophoresis methods after the treatment.

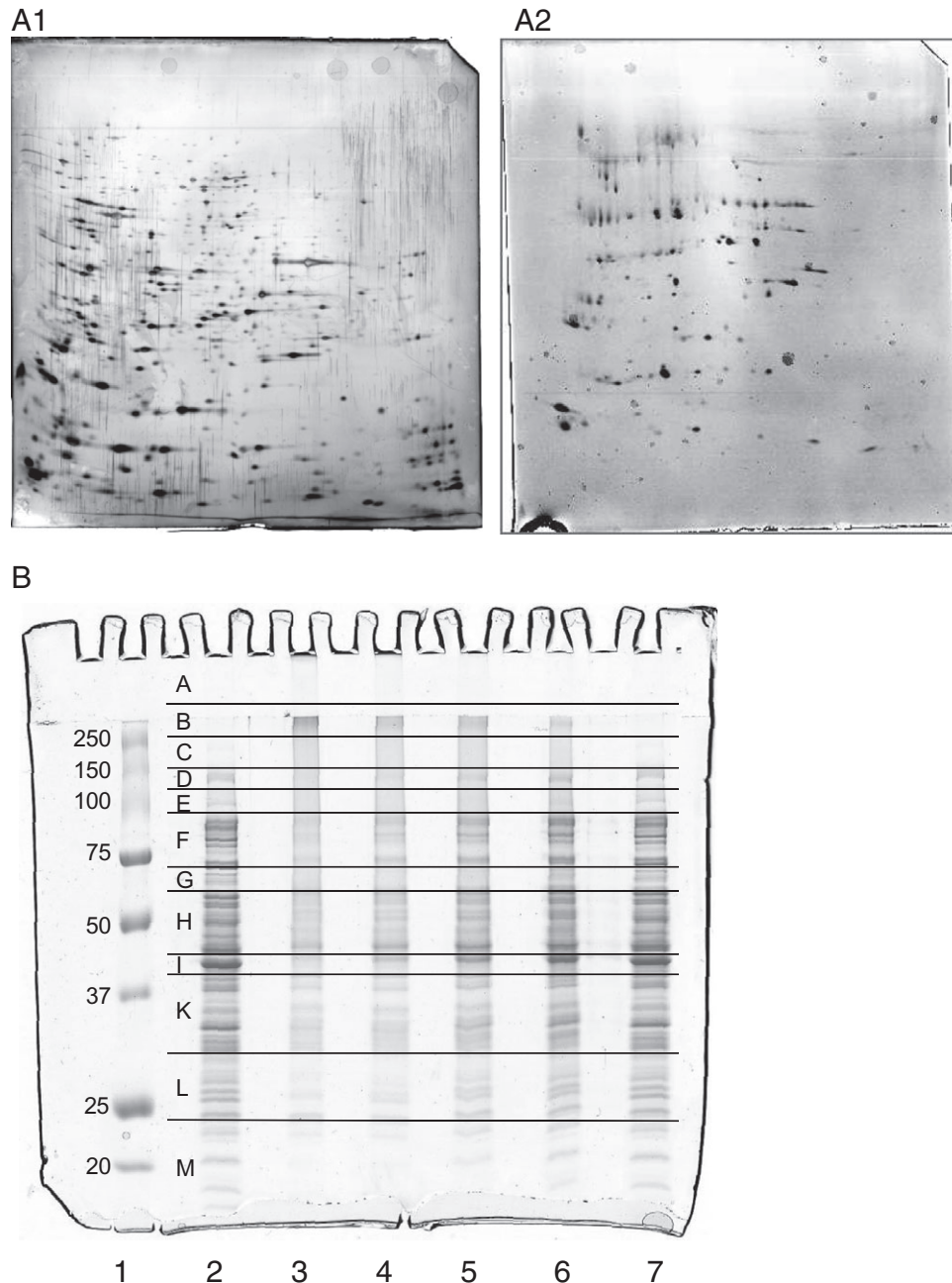


**Fig. 1.** One- and two-dimensional gel electrophoreses of UVA-irradiated *E. coli* samples and unirradiated dark controls.

A. Two-dimensional gel electrophoresis of unirradiated control (A1) and a sample irradiated with a fluence of 2200 kJ m<sup>-2</sup> (A2).

B. One-dimensional SDS-PAGE with protein standard ladder (lane 1; 250, 150, 100, 75, 50, 37, 25, 20 kDa), unirradiated control (lane 2), and irradiated samples with fluences of 2750 kJ m<sup>-2</sup> (lane 3), 2200 kJ m<sup>-2</sup> (lane 4), 1650 kJ m<sup>-2</sup> (lane 5), 1100 kJ m<sup>-2</sup> (lane 6), 550 kJ m<sup>-2</sup> (lane 7).

Experiments were performed at least three times; representative results are shown. In (A), 150 µg of cellular protein was loaded per gel. In (B), 15 µg of cellular protein was loaded onto gels per lane.

With the aim to identify damaged proteins, we first tried to compare unirradiated and irradiated cell samples on high-resolution 2D gels. Surprisingly, a massive loss of protein spots (70%), smearing and shifting of protein spots in irradiated samples as compared with the unirradiated control was observed (Fig. 1A and B). This effect was

reproducible. The shifting of protein spots of a similar molecular weight along the isoelectric focusing dimension was described before as 'protein stuttering' due to mistranslation (Ballesteros *et al.*, 2001), in our case the alteration in amino acid side-chains probably led to similar effects. Furthermore, on 1D gels, a smearing of protein

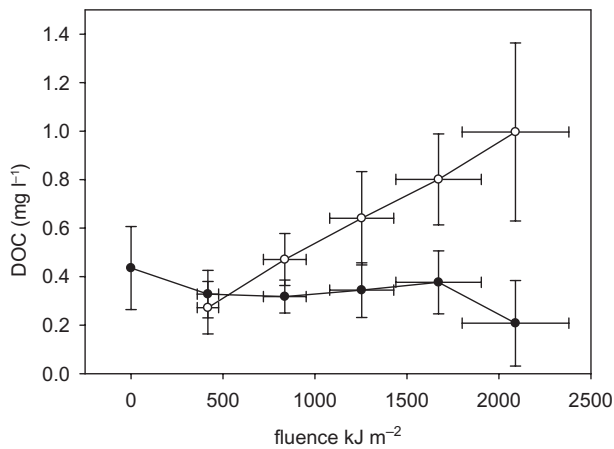


**Fig. 2.** Leakage of carbon compounds from *E. coli* cells after irradiation with different doses of UVA light. Immediately after exposure of cells ( $2 \times 10^8$  cells ml<sup>-1</sup>) to light, they were removed by filtration and the carbon released was measured in the medium using DOC analysis. (○) Irradiated samples; (●) non-irradiated controls.

bands was observed starting at an irradiation dose of around 1000 kJ m<sup>-2</sup> (Fig. 1B, lane 6) and this effect became even more pronounced with increasing irradiation doses. Gels were prepared with a reducing agent (DTT) and SDS as a detergent and therefore only covalently cross-linked aggregates would stick together whereas S-S bridges or hydrophobic interactions would be solubilized (Davies, 1987; Lund *et al.*, 2008). High irradiation doses made this effect even more pronounced (Fig. 1B, lane 3), with a loss of cellular protein and the formation of a new 'band' at the transition from the stacking to the separating gel.

#### DOC measurements of irradiated whole cells

Since many protein spots were missing on 2D gels and an obvious decrease in proteins resolved on 1D gels of irradiated cells was observed also, DOC was measured in supernatants of irradiated cells immediately after exposure to be able to exclude the possibility of cellular protein loss during irradiation. The cell concentration used in these experiments ( $2 \times 10^8$  cells ml<sup>-1</sup>) corresponds to a dry weight of about 56 µg ml<sup>-1</sup>, from which only about 1 µg ml<sup>-1</sup> cellular C was lost with increasing UVA irradiation (Fig. 2). As a cell contains about 50% C (28 µg ml<sup>-1</sup>) this corresponds to a loss of cellular C into the supernatant of about 2.8%. Even if this C exclusively originated from cellular protein (and not other cell components like metabolites, DNA, lipids or polysaccharides), this loss would only account for about 5.5% of the whole cellular protein content, since proteins on average consist of 46% C (Neidhardt *et al.*, 1990).

#### Quantitative aggregation effect on whole cell protein content

Since above results indicated that proteins seemed to stay within the cells, we tested whether it would be possible to quantify a protein aggregation effect that obviously led to the 'protein loss' observed on gels. Therefore, cells were broken up and the protein content of the whole cell extract was assessed after increasing times of mild centrifugation. During mild centrifugation, only larger insoluble particles settled whereas fully soluble proteins stayed in solution and therefore accounted for the protein content of the whole cell extract. When applying irradiation doses of 1000 kJ m<sup>-2</sup> and higher, larger protein aggregates were formed that sedimented, reaching as much as 80% of the total protein (Fig. 3). Interestingly, also the total protein content in the non-centrifuged whole cell lysate was decreasing to about 60% during irradiation, while the cell disruption efficiency still stayed between 97% and 99%. This might be due to amino acid modifications that alter the staining properties of proteins. This can be concluded from the fact that hardly any DOC leaked from irradiated cells and therefore proteins were still in the whole cell extract but not stainable anymore.

#### Identification of aggregation target proteins on 1D SDS-PAGE

As an alternative to 2D gels, we identified proteins affected by UVA light with the help of 1D gels. Samples irradiated with a dose of about 1000 kJ m<sup>-2</sup> and unirradiated controls were separated by 1D SDS-PAGE. In order to reduce sample complexity, the gel lanes were cut in 12

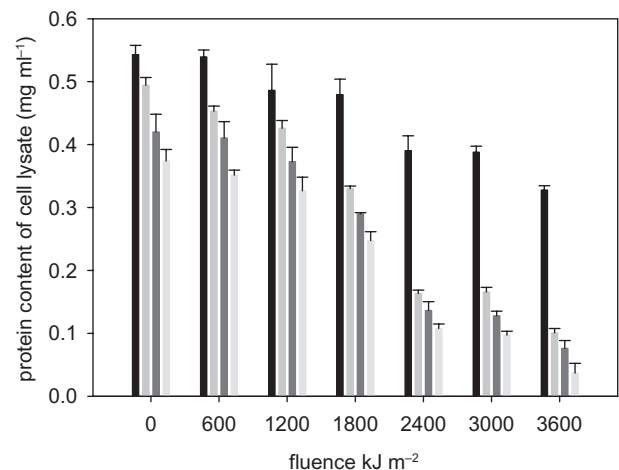


**Fig. 3.** Loss of whole cell protein by mild centrifugation: protein concentration in the whole cell lysate (black bar) and in the supernatants after 20, 40, 80 min of mild centrifugation at g-force of 16 000 (bars in medium, dark and light grey, respectively). A dark control was measured at the beginning (0 kJ m<sup>-2</sup>) and at the end (not displayed) of the experiment.

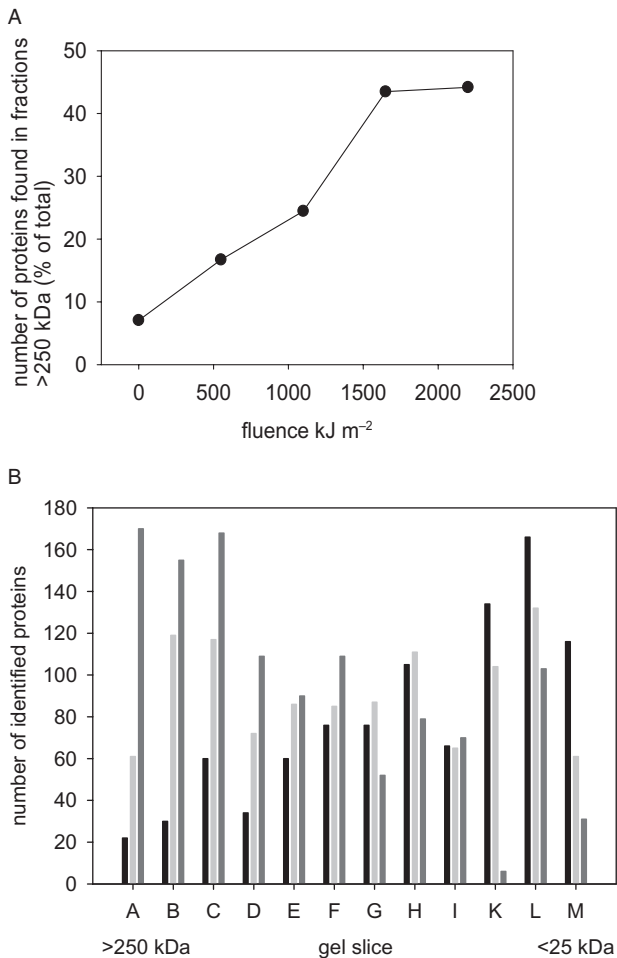


**Fig. 4.** The number of identified proteins increases in the gel cuts of the higher molecular weight range after cells have been irradiated.

A. Number of identified proteins in fractions of a molecular size of > 250 kDa, with increasing fluence.

B. Number of identified proteins in fractions of > 250 kDa to < 25 kDa. Shown are unirradiated samples (black) and irradiated samples at fluences of 1100 kJ m<sup>-2</sup> (light grey) and 2200 kJ m<sup>-2</sup> (dark grey). These results correspond to lane 1, 3 and 5 in Fig. 1B respectively).

gel slices (A–M) always containing proteins in the same molecular range (Fig. 1B). The proteins within these gel slices were then identified by tandem mass spectrometry. Interestingly, the number of proteins identified in the high molecular range, especially of the stacking gel and upper part of separating gel (containing proteins of a molecular weight > 250 kDa), was increasing with higher irradiation doses (Fig. 4A), reaching a maximum of 45% of all identified proteins present in these high-molecular-weight gel fractions. The same effect was visible when inspecting the whole molecular weight range [for the gel slices A (> 250 kDa) to M (< 25 kDa)], where an increase in the number of identified proteins is observed in the higher

molecular weight ranges, while the number decreases within the low molecular weight ranges (Fig. 4B).

#### Aggregation on single proteins evaluated by semi-quantitative spectral counts analysis

The spectral count is the number of unique peptides found for a particular protein. Assuming that the number of unique peptides is proportional to the amount of a protein in the original sample, spectral counts can be used as a semi-quantitative measure for the amount of the protein in the analysed sample. Here, the spectral counts were blotted for each individual protein against the corresponding molecular weight of the gel slices (A–M) to screen for possible mass shifts due to aggregation damages in the irradiated samples compared with the non-irradiated controls. For the 200 most abundant proteins, enough unique peptides were found to assess the original molecular weight of the protein and a possible mass shift after UVA irradiation due to aggregation or fragmentation. One example for a protein with a mass shift is the alpha-subunit of the F<sub>1</sub>F<sub>0</sub> ATPase (Fig. 5). Seventy-one of the 200 most abundant proteins of known function were aggregating reproducibly in three independent experiments. Their functions and the corresponding shifts are shown in Table 1. Many different cellular functions were affected in this way (Fig. 6).

#### Carbonylation damage to proteins

Oxidative carbonylation damage to proteins was observed very early during irradiation, and the pattern

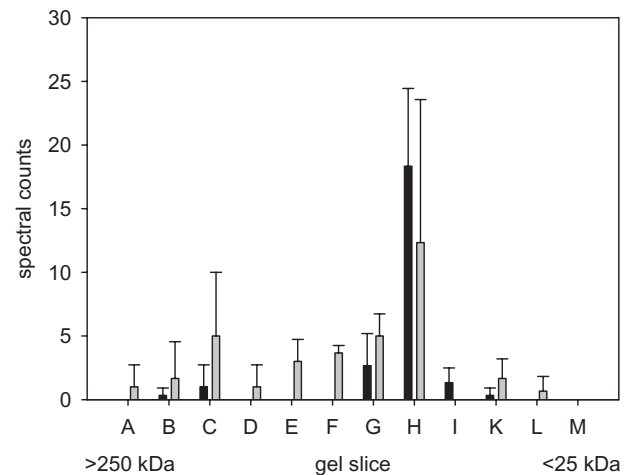


**Fig. 5.** Location of the alpha-subunit of the F<sub>1</sub>F<sub>0</sub>-ATPase in fractions of > 250 kDa to < 25 kDa, as an example for a protein that was found to aggregate during irradiation (1100 kJ m<sup>-2</sup>). Black bars represent distribution of the protein in the unirradiated sample, grey bars the irradiated sample. Error bars indicate standard deviations in spectral counts of a triplicate measurement.

**Table 1.** List of proteins found with a mass shift.

Protein name	Function	MW (kDa)	Found in gel slice (control)	Found in gel slice (irradiated)
RNA polymerase subunit beta	Transcription/transcription regulation	155	CDE	ABCDE
ATP-dependent protease Lon		87	F	BCDEF
Transcription termination factor Rho	Translation/protein biosynthesis	47	I	BCDEFHI
RNA polymerase sigma factor RpoD		70	F	BCEF
Elongation factor Tu		43	HIKLM	ABCDEFHIKLM
Elongation factor G		78	EFG	ABCDEF
Ribonuclease E		118	CDE	ABCDE
Translation initiation factor IF-2		97	EF	BCDEF
30S Ribosomal protein S1		61	FG	ABCDEF
Alanyl-tRNA synthetase		96	EF	ABCDEF
Glycyl-tRNA synthetase beta subunit		77	F	BCDEF
Threonyl-tRNA synthetase		74	F	BCDF
30S Ribosomal protein S7	20	M	BDELM	
Phenylalanyl-tRNA synthetase beta chain	87	F	BCEF	
50S Ribosomal protein L5	20	M	AM	
50S Ribosomal protein L6	19	M	ABCGM	
Magnesium-transporting ATPase	Transport/chemotaxis	99	CDEFGH	ABCDEF
Phosphoenolpyruvate-protein phosphotransferase		64	G	ABCDEF
Preprotein translocase subunit secA		102	EF	BCDEF
Acridiflavine resistance protein B		114	EF	BCDE
Acridiflavine resistance protein A precursor		42	I	BCDI
PTS system mannitol-specific EIICBA component		68	H	BCEFGH
PTS system glucose-specific EIICB component		51	IK	CDEFI
Ribonucleoside-diphosphate reductase 1 subunit alpha		86	EF	BCDEF
Carbamoyl-phosphate synthase large chain		118	CDE	ABCDE
Glutamine synthetase		52	GH	ABCDEF
Cysteine desulfurase	45	IK	ABCDI	
Tryptophanase	AA degradation	53	GHIKL	ABCDEFHIK
4-Aminobutyrate aminotransferase		46	HI	ABCDEFHIK
Bifunctional protein putA		144	DE	ABCDEF
Glycine dehydrogenase		104	EF	ABCDEF
Aminopeptidase N		99	G	ABCEG
Aspartate ammonia-lyase		52	H	ABCDEGH
Polyribonucleotide nucleotidyltransferase		77	F	BCDEF
3-Oxoacyl-facyl-carrier-protein] synthase 1		43	I	BCDEI
Inosine-5'-monophosphate dehydrogenase		52	H	BCDEGH
Bifunctional purine biosynthesis protein PurH		57	GH	BCDEGH

NADH-quinone oxidoreductase subunit G	100	EF	BCDEF	Respiration
ATPase subunit alpha	55	GHI	ABCDEFHGHIK	ATP synthesis
Enolase	46	HIKL	ABCDEGHK	Glycolysis
Fructose-bisphosphate aldolase class 2	39	BK	BEFGKL	
Pyruvate kinase II	51	H	BCDGH	
2-Oxoglutarate dehydrogenase E1 component	105	EF	ABCDEF	TCA
Pyruvate dehydrogenase E1 component	100	EF	ABCDEF	
Aconitate hydratase 2	94	EF	ABCDEF	
Succinate dehydrogenase flavoprotein subunit	64	FG	ABCDEF	
Dihydropyridyl dehydrogenase	51	H	ABCDEF	
Acetyl-coenzyme A synthetase	72	FG	ABCDEF	
Citrate synthase	48	HIKL	ABCDEFHGHIK	
Dihydrodipicolinate synthase component of pyruvate dehydrogenase complex	66	FG	ABCDEF	
Succinyl-CoA synthetase beta chain	41	IKL	ABCDEGHIK	
Dihydrodipicolinate synthase component of 2-oxoglutarate dehydrogenase complex	44	H	ABCDEF	
Formate acetyltransferase 1	85	FG	BCDEFG	Fermentation
Aldehyde-alcohol dehydrogenase	96	EFG	ABCDEF	Degradation of CH
Glucose-1-phosphatase	46	HI	CDEF	Glyoxylate cycle
Isocitrate lyase	72	HIKLM	ABCDEFHGHIKLM	Pentosephosphate pathway
Transketolase 1	73	F	BCFG	
Transketolase 2	60	GHL	BCDEF	Gluconeogenesis
Phosphoenolpyruvate carboxykinase [ATP]	87	G	BCDEF	
Phosphoenolpyruvate synthase	82	F	BCDEF	c4 metabolism
NADP-dependent malic enzyme	69	FG	ABCDEF	Chaperone
Chaperone protein DnaK	96	F	ABCDEF	
Chaperone protein ClpB	48	H	ABCDEF	
Trigger factor	71	FG	BCDFG	
Chaperone protein HtpG	80	F	BCDEF	Catalase
Peroxidase/catalase HPI	97	EF	BCDEF	DNA repair
DNA gyrase subunit A	90	F	BEF	
DNA gyrase subunit B	19	M	ACDEFHGKLM	Osmotic stress
DNA protection during starvation protein	21	M	ADEFHGKLM	Periplasm
Osmotically-inducible protein Y precursor	61	GH	ABCDEF	
Periplasmic oligopeptide-binding protein precursor	37	KL	ABCDEFHGHIK	
Outer membrane protein A precursor	37	K	ABCDEF	Unknown
csdI predicted protein	53	H	BCDEF	
Glutamate decarboxylase alpha			BCDEF	

These proteins were reproducibly aggregating in three independent experiments. Corresponding gel lanes are shown in Fig. 1A, lane 2 for control and lane 6 for irradiated samples (1100 kJ m<sup>-2</sup>).

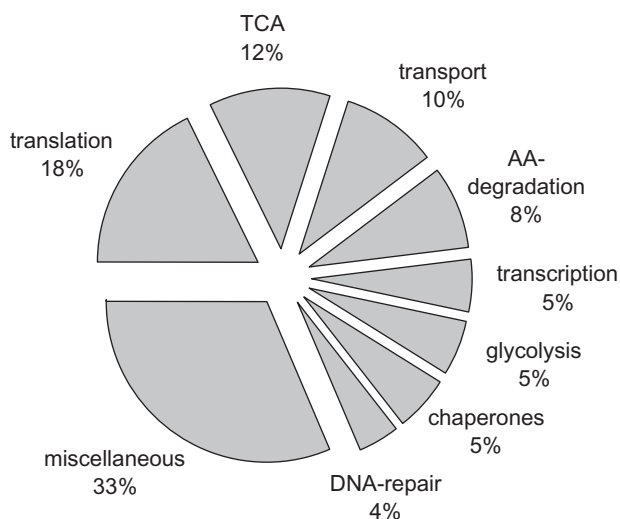


**Fig. 6.** Cellular functions of the 71 proteins found with a mass shift (corresponding to 100%) out of the 200 most abundant *E. coli* proteins identified by MS/MS.

was not changing thereafter (Fig. 7). Overall, carbonylation damage increased 3.5-fold when compared with dark controls in samples irradiated with  $645 \text{ kJ m}^{-2}$ , and 7.5-fold when irradiated up to  $2500 \text{ kJ m}^{-2}$  (Tables 2 and 3 respectively). The bands on the Western blot seemed to be rather specific up to an irradiation dose of  $950 \text{ kJ m}^{-2}$ , which corresponds to the dose where the cells started dying off when plated on TSA agar. Two reproducible bands around 78 kDa and 55 kDa were found with the carbonylation immunoblot method already with an irradiation dose of  $215 \text{ kJ m}^{-2}$  and a third band of about 35 kDa was appearing with irradiation doses of  $645 \text{ kJ m}^{-2}$  and more (Fig. 7A). In the high molecular weight range ( $> 170 \text{ kDa}$ ) a pronounced accumulation of carbonylated sites was detected (Fig. 7A) and with irradiation doses higher than  $950 \text{ kJ m}^{-2}$  a general 'smearing' similar to the one on SDS-PAGE was visible on the blots as well (Fig. 7B and C), both indicating a high amount of carbonylation sites in aggregating proteins. The identification of carbonylated proteins after UVA irradiation turned out to

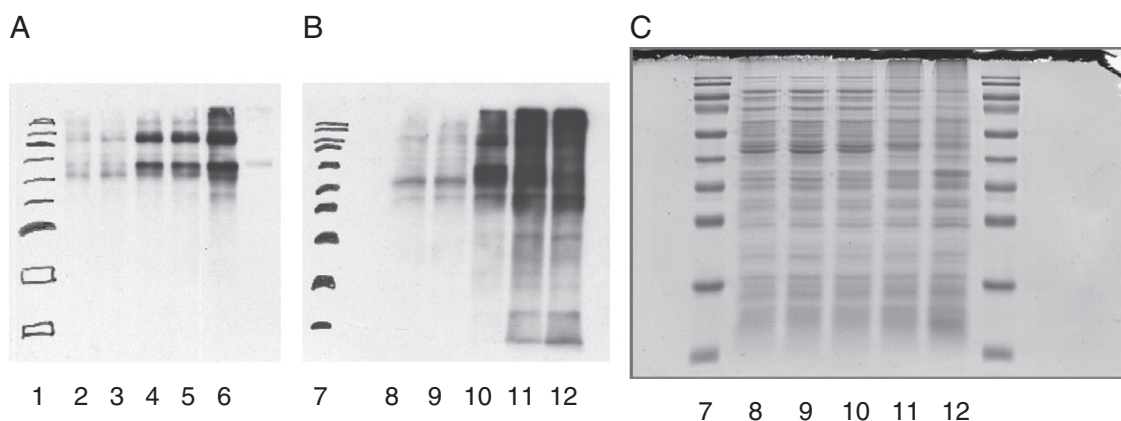


**Fig. 7.** Specific carbonylation of distinct protein bands at molecular weight ranges around 78 kDa, 55 kDa and 35 kDa occurs very early during irradiation.

A. Oxyblot on whole cell extract with low fluences. Protein standard ladder (lane 1; 170, 130, 95, 72, 55, 43, 34, 26, 17, 10 kDa), dark controls (lanes 2 and 3),  $215 \text{ kJ m}^{-2}$  (lane 4),  $430 \text{ kJ m}^{-2}$  (lane 5),  $645 \text{ kJ m}^{-2}$  (lane 6).

B. Oxyblot on whole cell extract with high fluences. Protein standard (lane 7), dark controls (lanes 8 and 9),  $950 \text{ kJ m}^{-2}$  (lane 10),  $1900 \text{ kJ m}^{-2}$  (lane 11),  $2500 \text{ kJ m}^{-2}$  (lane 12).

C. One-dimensional SDS-PAGE of samples shown in (B).

Experiments were performed at least three times, representative results are shown.

**Table 2.** Carbonyl content in cell extracts of unirradiated and irradiated samples with a dose corresponding to less than 1 h of natural sunlight irradiation (see Fig. 7A for corresponding blot).

Fluence ( $\text{kJ m}^{-2}$ )	Amount of protein ( $\mu\text{g}$ )	Density ( $\text{OD mm}^{-2}$ )	Density/protein ( $\text{OD mm}^{-2} \mu\text{g}^{-1}$ )	Increase (fold)
0 (beginning)	7.5	29	3.86	1
0 (end)	7.5	31.13	4.15	1.08
215	7.5	52.08	6.94	1.8
430	7.5	53.9	7.19	1.86
645	7.5	103.92	13.86	3.59

Computerized densitometry was performed on films exposed for 30 s to the membrane during chemiluminescent detection of carbonyl groups. Afterwards the density per  $\mu\text{g}$  of loaded protein and the increase in each sample compared with the first unirradiated control cell extract were calculated.

**Table 3.** Carbonyl content in cell extracts of unirradiated and irradiated samples corresponding to about 5 h of natural sunlight irradiation (see Fig. 7B for corresponding blot).

Fluence (kJ m <sup>-2</sup> )	Amount of protein (µg)	Density (OD mm <sup>-2</sup> )	Density/protein (OD mm <sup>-2</sup> µg <sup>-1</sup> )	Increase (fold)
0 (beginning)	14.79	53.25	3.6	1
0 (end)	15.22	57.11	3.75	1.04
950	15.02	132.52	8.82	2.45
1900	14.9	211.36	14.19	3.4
2500	7.35	193.25	26.29	7.3

Computerized densitometry was performed on films exposed for 30 s to the membrane during chemiluminescent detection of carbonyl groups. Afterwards the density per µg of loaded protein and the increase in each sample compared with the first unirradiated control cell extract were calculated.

be challenging. Two different approaches were taken. First, samples were run on 2D gels with the intention to do immunoblotting, as reported before (Dukan and Nystrom, 1999). However, proteins of irradiated cells shifted so strongly that the picture was not comparable to the original pattern anymore (Fig. 1A2). Second, carbonylated proteins were labelled with biotin-hydrazine with the intention to specifically enrich them by avidin for further analysis on SDS-PAGE and tandem mass spectrometry (Mirzaei and Regnier, 2005). However, this affinity enrichment was not as selective as expected, be it due to non-specific background biotinylation within our samples, be it due to protein aggregation making the specific enrichment difficult. Nevertheless, we tried to identify probable candidates for early carbonylation targets with two criteria. First, they needed to have a molecular size in the range of the positively stained oxyblot bands and second, they needed to show mass shifts making them suspicious to contain newly introduced carbonylation sites. Putative carbonylation candidates singled out in this way were elongation factor G (EFG 78 kDa), 60 kDa chaperonin (GroL 57 kDa), ATPase subunit alpha (ATPA 55 kDa), ATPase subunit beta (ATPB 50 kDa), Lysyl-tRNA synthetase (SYK2 58 kDa), glutamine synthetase (GLNA 52 kDa), 50S ribosomal protein L2 (RL2 30 kDa), outer membrane protein A (OMPA 37 kDa) and transaldolase B (TALB 35 kDa).

## Discussion

### *Protein oxidation and carbonylation patterns*

There are many different pathways that introduce carbonylation sites into proteins (Levine and Stadtman, 2001). The extent of protein carbonylation in biological samples is indicative for the level of oxidation processes that happen to cellular protein during a certain treatment or senescence. Oxidized proteins are non-functional and lose their structural or enzymatic function. It is believed that a high level of oxidized proteins causes substantial disruption of cellular functions. Carbonylated proteins cannot be repaired, and have to be degraded. If not degraded immediately, they tend to form covalent cross-

links with other proteins and finally aggregate. Therefore, the increased smearing on immunoblots for fluences > 950 kJ m<sup>-2</sup> could originate either from only a few proteins that were specifically carbonylated at lower fluences and then spread over a wider molecular weight range prior to blotting due to aggregation, or from a diversification of protein carbonylation targets with increasing irradiation dose.

A number of authors have reported increased carbonylation levels with ageing, starvation and different stresses. As in the case of UVA irradiation, these do not affect the proteome uniformly. Some of the damaged proteins were found to be major targets in studies on senescence and oxidative stress, too. For example, elongation factor G, glutamine synthetase, 60 kDa chaperonin (Dukan and Nystrom, 1998; 1999; Tamarit *et al.*, 1998), and outer membrane protein A and ATPase beta chain were reported to be affected, which corresponds to our observation on probable carbonylation candidates (Cabisco *et al.*, 2000). This suggests that the oxidative damage to the proteome is quite specific in all cases of increased oxidative stress and senescence, and, furthermore, that UVA light is acting via production of oxidative radicals and causes oxidative stress to the cell. Still, it is not clear how the level of carbonylation affects the viability of cells. Yeast cultures were reported to survive up to 10% of their proteome being irreversibly oxidized (Mirzaei and Regnier, 2006a). But dependent on how essential the function of a targeted protein is, e.g. if there are no isoenzymes that can replace it in the meantime for its function, carbonylation may be lethal. With essential functions of the energy metabolism targeted during SODIS (ATPase subunits alpha and beta) and the targets in the translation apparatus (elongation factor G, lysyl-tRNA synthetase, 50S ribosomal protein L2), a loss of viability due to carbonylation is probable. Protein modification is often accompanied by other cellular damages. For example, in brain cell mitochondria, where respiration was inhibited, membrane potential and enzyme activities were reduced, ROS levels were elevated and the antioxidant defence system was decreased (Long *et al.*, 2009). It is likely that these effects influence each other, leaving us with the

crucial question of what is the causative elicitor for the cellular damages, or in other words, which one was the 'chicken' and which ones are just 'eggs'. We believe that protein oxidation might be the elicitor for further cellular effects in the case of UVA irradiation, simply because it was observed very early during the inactivation process.

#### *Aggregation (and in some cases fragmentation) of proteins during SODIS*

It is widely accepted that enzymes with active-site iron-sulfur clusters are highly sensitive to inactivation by oxygen radicals (Gardner and Fridovich, 1991). One of these enzymes is aconitase of *E. coli*, involved in iron pool regulation within the cell (Varghese *et al.*, 2003). Indeed, we do find this enzyme aggregated in our experiments. This again corroborates the presumption that UVA light acts via reactive oxygen. Aggregation is a direct consequence of protein oxidation. Our data clearly demonstrate that many different proteins within the cell are heavily affected by aggregation at an irradiation dose of about 1000 kJ m<sup>-2</sup>, which corresponds to about 2 h of natural sunlight and a 99% reduction in colony-forming units (cfu) when plating the cells on TSA agar. The capacity of the cellular quality control system by chaperones therefore seems to be exceeded at this point. The cell's depletion in ATP that occurs right at the beginning of the irradiation process (Berney *et al.*, 2006; Bosshard *et al.*, 2009b) may be one cause for ATP-dependent chaperones not being able anymore to successfully fight protein misfolding and aggregation. For covalent protein cross-linking, protein oxidation damages (such as carbonylations) are an indispensable prerequisite. With such a wide variety of targeted proteins, impairing many different physiological functions within the cell, and such a high quantity of protein aggregates as we observed in our experiments, it is hard to imagine that cells could recover from the UVA-induced damage. Nevertheless, some authors propose that initially, protein aggregation may be cytoprotective by sequestering non-functional proteins away from the cellular metabolism at specific sites and thereby also facilitating the recruitment of components of the cellular defence response (Maisonneuve *et al.*, 2008c). Moreover, a small amount of aggregating proteins were found even in exponentially growing (so to say 'young') cells, which means that protein aggregation *per se* is not lethal as long as it does not exceed the cells capacity to deal with the phenomenon. But the level of damaged and aggregated proteins significantly increased in ageing bacterial populations during stationary phase and extensive protein aggregation might impair cell viability, e.g. by trapping other molecules (Wickner *et al.*, 1999). With a wide variety of vital cellular functions hampered by aggregation, many secondary

effects on cell physiology can be expected. Particularly important are probably the transcription and translation apparatus, transport systems, amino acid synthesis and degradation, respiration, ATP synthesis, glycolysis, the TCA cycle, chaperone functions and catalase. It is very likely that the lack of these functions directly impairs cellular viability during UVA irradiation.

Many enzymes may also be affected at fluences higher than 1000 kJ m<sup>-2</sup>. For example, glyceraldehyde-3-P dehydrogenase was recently used as a model for environmentally induced protein damage (Voss *et al.*, 2007). These authors found that UVA decreased the free thiol content, which indicates that the intracellular redox balance was disturbed. The enzyme's activity consequently decreased to 10% with about 1000 kJ m<sup>-2</sup>, which is comparable to our results (Bosshard *et al.*, 2009a). Aggregation and fragmentation effects were found only with fluences > 2000 kJ m<sup>-2</sup>. This is comparable to our results presented here, where aggregation of glyceraldehyde-3-P dehydrogenase was only seen at a fluence corresponding to about 2000 kJ m<sup>-2</sup> (data not shown), but not at 1000 kJ m<sup>-2</sup>. But since culturability of cells shows a massive drop at about 1000 kJ m<sup>-2</sup>, applying higher fluences might be beating a dead horse. Other authors described that application of a lethal UVA dose shifted the location of HPI and HPII on gels, likely as cause of aggregation (Hoerter *et al.*, 2005b).

#### *Defence against protein carbonylation and aggregation by chaperones and degradation enzymes*

Proteins in a cell are affected by reversible and irreversible damage. Unwanted disulfide bond formation ('disulfide stress') influences the folding of proteins within the cell, but it is reversible by glutathione and chaperones. Irreversible is the oxidation of amino acid residues by metal ion-catalysed oxidation reactions, leading (among other modifications) to protein carbonylation. Protein oxidation seems to enhance the ability of the cell to selectively degrade the affected protein. Therefore, some authors argued that carbonylation might be tagging a protein as a sign to the degradation machinery (Nyström, 2005). It was reported that *E. coli* has specific proteases that selectively degrade oxidized proteins in an ATP-independent pathway (Davies and Lin, 1988). In this way the cells can circumvent the problem of ATP depletion in many situations of physiological stress. In contrast to this, chaperone systems usually depend on ATP for functioning, such as the DnaK/DnaJ/GrpE system that helps most proteins during folding. For *E. coli* exposed to oxidative stress, which was associated with ATP depletion, Hsp33 was induced and replaced the DnaK system (Winter *et al.*, 2005). In this situation, DnaK was inactivated because its N-terminus becomes labile. Other authors claimed that

Hsp33 is induced by disulfide formation under oxidative stress (Jakob *et al.*, 1999; 2000). Either way, Hsp33 was not induced to measurable amounts in our experiments because we worked with starved cells that are unable to induce much *de novo* protein synthesis. Therefore, the DnaK system is still the more relevant in our case. Since a massive ATP depletion during UVA treatment was observed, it seems logical that DnaK and its substrate proteins (Winter *et al.*, 2005) are targeted by aggregation processes, and this is indeed what we were able to observe here. We found 11 of 39 DnaK substrate proteins aggregated, namely aldehyde-alcohol dehydrogenase, outer membrane protein A, aconitate hydratase 2, threonyl-tRNA synthetase, transketolase 1, pyruvate dehydrogenase, 2-oxoglutarate dehydrogenase E1 component, succinate dehydrogenase flavoprotein subunit, transcription termination factor rho, cysteine desulfurase, 3-oxoacyl-(acyl-carrier-protein) synthase 1. Also DnaK itself and other chaperones (ClpB, HtpG) were found to aggregate, and one must expect that this will even accelerate the process of protein aggregation during UVA treatment.

#### *Consequences of observed protein damages for the cell*

Carbonylation and aggregation of proteins affect a wide spectrum of structural and enzymatic proteins within the cell. Vital cellular functions like the transcription and translation apparatus, transport systems, amino acid synthesis and degradation, respiration, ATP synthesis, glycolysis, TCA, chaperone functions and catalase are targeted by UVA irradiation. With the loss of catalase function, the cell loses its first line of defence against ROS, rendering the cell more susceptible against oxidative stress. A second line is lost by non-functional chaperones (be it due to lack of ATP to fuel chaperone function, be it due to aggregation of chaperones), which would be able to prevent protein aggregation. Moreover, damage to translational proteins reduces the cells ability to replace damaged proteins with new ones. The translation apparatus was a target of aggregation effects also in other studies (Mirzaei and Regnier, 2005; 2006a,b; 2007). The proteins in the translation apparatus are very closely associated and therefore might be especially susceptible to aggregation. Moreover, an important protein for DNA protection and repair, Dps, was found to be damaged in our study. Dps (DNA protection under stationary phase) usually is induced with nutritional stress during stationary phase and under oxidative stress. It carries out two functions. First, it physically protects DNA from oxidative damage and additionally maintains a low level of gene expression. Second, the structure of Dps is similar to ferritin and it was suggested that iron sequestration helps in protecting the DNA (Grant *et al.*, 1998). Hence, its close association with iron might

enhance photo-Fenton reactions during UVA irradiation and aggregation of the protein.

#### *Accelerated senescence due to UVA stress*

It was a long-standing belief that bacteria are not ageing and that growing bacterial populations are not age structured. However, it has been recognized in the last years that even if bacterial populations are able to grow 'eternally', individual bacterial cells indeed are ageing, i.e. they slow down in their ability to divide and finally stop reproduction (Ackermann *et al.*, 2003; Stewart *et al.*, 2005; Nyström, 2007; Lindner *et al.*, 2008). Signs of ageing have also been observed in stationary-phase cells. The carbonylation pattern of non-growing cells shows that the cells get dysfunctional in many respects (Desnues *et al.*, 2003; Nyström, 2003; 2005; 2006; 2007). In ageing cells, at least one out of every three proteins carries a carbonyl group, and this level of dysfunctional proteins is believed to be sufficient that carbonylation can be considered not only as a marker of ageing, but also as a cause for the cellular changes during ageing (Levine and Stadtman, 2001; Terman and Brunk, 2006). The pattern of carbonylation during ageing reminds of the pattern we observed with UVA treatment. Accumulation of protein oxidation and protein aggregates has been described as a sign and a cause for cellular ageing by many authors (Grune *et al.*, 2004; Stadtman, 2006; Terman and Brunk, 2006; Maisonneuve *et al.*, 2008a). We believe that UVA damages probably go back to a very similar cell damage mechanism also met during ageing and oxidative stress in cells. UVA irradiation probably accelerates the processes observed during cellular ageing.

## **Experimental procedures**

### *Bacterial strains, growth media and cultivation methods*

In all experiments wild-type *E. coli* K12 MG1655 was used from cryo-cultures and for each experiment loop-streaked onto a new TS agar plate. For batch cultivation, LB broth (10 g of tryptone, 5 g of yeast extract, 10 g of NaCl, per litre) was filter-sterilized with Millipore syringe filters (Millex GP, 0.2 µm) and diluted to one-third of its original strength. Erlenmeyer flasks containing 20 ml of diluted LB were inoculated with a single colony and incubated at 37°C with vigorous shaking until the cells reached exponential growth (OD<sub>546</sub> between 0.1 and 0.2). Then the culture was diluted to an OD<sub>546</sub> of 0.002 into 150 ml of pre-warmed diluted LB in a 1000 ml Erlenmeyer flask and shaken overnight for 18 h until stationary phase was reached. Stationary phase was confirmed with five consecutive OD<sub>546</sub> measurements.

### *UVA exposure*

Cells were harvested by centrifugation at 16 000 *g* for 15 min and washed three times with filter-sterilized still mineral

water. The pellet was suspended in filter-sterilized mineral water to reach an  $OD_{546}$  of 2.2 ( $1-5 \times 10^9$  cells  $ml^{-1}$ ) in order to obtain a high enough protein concentration. Cell suspensions were incubated for 1 h at 37°C to allow the cells to adapt to the mineral water. Aliquots of 20 ml of cell suspension were exposed to UVA light in 30 ml quartz glass tubes. The tubes were placed in a carousel reactor (Wegelin *et al.*, 1994) equipped with a medium-pressure mercury lamp (TQ 718), which was operated with 500 W. The light emitted from the lamp passed through the glass jacket and through a filter solution before reaching the cells in the quartz glass tubes. The filter solution, consisting of 12.75 g  $l^{-1}$  of sodium nitrate (cut-off at 320 nm), was used to obtain a UVA light spectrum comparable to solar light. The temperature of the filter solution was maintained at 37°C during the experiments. The fluence rates at the position of the tubes were determined during every experiment by using actinometry (Wegelin *et al.*, 1994). For each experiment, a part of the bacterial suspension was kept at 37°C as a dark control.

#### Whole cell extract

Triplicate samples (irradiated at 1000  $kJ\ m^{-2}$  and non-irradiated) with a sample volume of 20 ml and a concentration of  $1-5 \times 10^9$  cells  $ml^{-1}$  were harvested by centrifugation at 16 000 g for 15 min, resuspended in 3 ml of lysis buffer [10 mM Hepes pH 7, 0.1% CHAPS, 1× Protease inhibitor (complete, Roche, Mannheim, Germany)] and disrupted by one passage through a pre-cooled French press at 15 000 p.s.i. Cell disruption efficiency with one passage through the French press was always > 97% in non-irradiated and irradiated samples as evaluated by microscopy and flow cytometric total cell counts. Unbroken cells were then removed by centrifugation for 15 min at 16 000 g and glycerol was added to a final concentration of 5%. Samples were rapidly frozen in liquid  $N_2$  and stored at -20°C. Protein concentration was measured by the Bradford method (Bradford, 1976).

#### 1D SDS-PAGE combined with LC-MS/MS

Whole cell extracts were separated by SDS-PAGE (Laemmli, 1970) using 12% polyacrylamide gels and stained by Coomassie (Gallagher, 2006). Protein lanes were cut in 12 horizontal gel slices (A–M), which contained approximately the same amount of protein. Proteins were immediately subjected to in-gel tryptic digestion (Shevchenko *et al.*, 1996). The resulting peptide mixtures were analysed on a hybrid LTQ-Orbitrap mass spectrometer (ThermoFischer Scientific, Bremen, Germany) interfaced with a nanoelectrospray ion source. Chromatographic separation of peptides was achieved on an Eksigent nano LC system (Eksigent Technologies, Dublin, CA, USA), equipped with a 11 cm fused silica emitter, 75  $\mu m$  inner diameter (BGB Analytik, Bockten, Switzerland), packed in-house with a Magic C18 AQ 3  $\mu m$  resin (Michrom BioResources, Auburn, CA, USA). Peptides were loaded from a cooled (4°C) Spark Holland auto-sampler and separated using an acetonitrile/water solvent system containing 0.1% formic acid at a flow rate of 200  $nl\ min^{-1}$  with a linear gradient from 3% to 35% acetonitrile in 60 min. Up to

six data-dependent MS/MS spectra were acquired in the linear ion trap for each Fourier-transform (FT)-MS spectral acquisition range. The latter was acquired at 60 000 full-width half-maximum (FWHM) nominal resolution settings with an overall cycle time of approximately 1 s. Charge state screening was employed to select for ions with two charges and rejecting ions in single-charge state. The automatic gain control (AGC) was set at  $5e^5$  for ion injection control and at  $1e^4$  for full FT-MS and linear ion trap MS/MS. The instrument was calibrated externally according to the manufacturer's instructions. All samples were acquired using internal lock mass calibration on  $m/z$  429.088735 and 445.120025.

#### Database searches, data validation and protein quantification

The Mascot Search Engine (version No. 2.2.04) was used for protein database searches against the Swissprot reference database. MS/MS ion searches were performed with the following settings: (i) trypsin was chosen as protein-digesting enzyme and up to two missed cleavage sites were tolerated, (ii) carbamidomethylation of cysteine was chosen as fixed modification, and (iii) oxidation of methionine and formation of pyro-glutamic acid from glutamine and glutamic acid were chosen as variable modifications. Searches were performed with a parent ion mass tolerance of 5 ppm and a fragment ion mass tolerance of 0.8 Da. Scaffold (version 2.05.01, Proteome Software, Portland, OR, USA) was used to validate and quantify MS/MS-based peptide and protein identifications. Peptide identifications were accepted if they could be established at greater than 95.0% probability as specified by the Peptide Prophet algorithm (Keller *et al.*, 2002). Protein identifications were accepted if they could be established at greater than 99.0% probability and contained at least one identified peptide. Protein probabilities were assigned by the Protein Prophet algorithm (Nesvizhskii *et al.*, 2003). Proteins that contained similar peptides and could not be differentiated based on MS/MS analysis alone were grouped to satisfy the principles of parsimony. Semi-quantitative analyses of protein abundances were performed on the basis of the number of unique peptides that were assigned to a protein by the Scaffold software (= spectral counts). The spectral counts were then blotted for each individual protein against the molecular sizes of the gel pieces (A–M). For the 200 most abundant proteins, enough unique peptides were found to assess the original molecular weight of the protein and a possible shift after UVA irradiation due to aggregation or fragmentation. Carbonylation sites were found by filtering results for amino acid mass shifts of +15.999 for the conversion of proline to glutamic semialdehyde, -43.071 for the conversion of arginine to glutamic semialdehyde and -1.031 for the conversion of lysine to amino adipic semialdehyde (Requena *et al.*, 2003).

#### Immunoblot against carbonylation sites

Western blotting was performed to detect carbonylated proteins using the Oxyblot™ Protein Oxidation Kit (Millipore, Chemicon, Zug, Switzerland) according to the manual. The samples containing 7.5 or 15  $\mu g$  of protein were subjected to

2,4-dinitrophenylhydrazine (DNPH) to derivatize carbonylation sites to 2,4-dinitrophenylhydrazone. Solutions for negative control samples lacked DNPH. After 15 min exposure to the derivatizing reagent a neutralization solution was added until a stable change in colour from yellow to red was observed. The DNPH-derivatized protein samples were separated by 12.5% or 8% SDS-PAGE and blotted onto nitrocellulose membranes (Bio-Rad, Reinach, Switzerland). The membranes were blocked with 1% of bovine serum albumin (BSA) and PBS-T and incubated with primary antibodies against DNP in 1% BSA in PBS-T for 1 h at room temperature. This was followed with a horseradish-peroxidase antibody conjugate directed against the primary antibody for 1 h at room temperature. The chemiluminescent visualization was carried out as described earlier (Shacter *et al.*, 1994). After the exposure to the film the membrane was incubated with chromogenic BM Blue POD substrate (Roche, Rotkreuz, Switzerland). Like this it was possible to assemble the film on the membrane and draw the pre-stained molecular weight (MW) marker onto the film. This step was necessary because the carbonylated MW marker provided by Chemicon was not consistently detectable and the obtained pattern could not always be related to the MWs given in the protocol. Computerized densitometry was performed using a GS-800 calibrated Densitometer with the 1D Analysis software Quantity one® (both from Bio-Rad).

#### Centrifugable aggregates by 'mild centrifugation'

As reported recently (Maisonneuve *et al.*, 2008a,c), we separated cellular protein aggregates from whole cell extracts obtained by French press with relatively mild centrifugation (16 000 g) and measured the protein content of the supernatant at different time points after onset of centrifugation. Protein loss in the supernatant was interpreted as protein loss due to sedimentation of insoluble proteins in the form of large aggregates.

#### DOC measurements

UVA irradiation with  $2 \times 10^8$  cells ml<sup>-1</sup> was performed as described above. Immediately after exposure to light cells were removed by filtration through pre-washed 0.22 µm filters. DOC was then measured on a SHIMADZU TOC-5050A analyser with a highly sensitive catalyst as non-purgeable organic carbon (NPOC).

#### 2D gel electrophoresis

Samples of 1 ml with a concentration of  $1-5 \times 10^9$  cells ml<sup>-1</sup> were removed from the quartz glass tubes or from dark controls, transferred into Eppendorf tubes which were placed on ice, cells were spun down at 4°C (16 000 g) and the pellet was resuspended in 50 µl of lysis buffer I (stock solution composition: 50 µl of 0.5 M Tris-HCl pH 6.8, 80 µl of 15% SDS, 20 µl of glycerol, 40 µl of beta-mercaptoethanol and 270 µl of nanopure H<sub>2</sub>O). Cells were incubated for 4 min at 95°C, followed by 1 h of shaking at 37°C. After incubation, 50 µl of lysis buffer II (9.5 M Urea, 0.04% Nonidet P40 and 5% beta-mercaptoethanol) was added, the sample was fast-

frozen (liquid nitrogen) and stored at -80°C until gel electrophoresis was performed. To each sample 50 U of benzoase (Merck KGaA, Darmstadt, Germany) was added and nucleic acids digestion was performed for 1 h at 37°C. Protein concentration was measured using Bio-Rad Protein Assay Kit; 200 µg of proteins were added to rehydration buffer (accordingly to the manufacturer) adjusted to an end volume of 330 µl and used to rehydrate ReadyStrip pl 3-10 (Bio-Rad, Basel, Switzerland). Active rehydration was performed with IEF-Cell (Bio-Rad) for 12 h at 50 V, followed by isoelectric focusing at 9000 V until 60 000 V·h was reached. Equilibration and transfer to the second dimension were performed according to the manufacturer (Bio-Rad). SDS-PAGE was performed on acrylamide gels (12.5%) using PROTEAN II MULTI-CELL (Bio-Rad). Gel images were scanned with the GS-800 Calibrated Densitometer (Bio-Rad) and the obtained images were analysed with the PDQuest Basic software version 8.0 (Bio-Rad) (Franchini, 2006).

#### Acknowledgements

This project was financially supported by the Velux Foundation (project No. 346). We thank Marc Suter, Holger Nestler and Victor Nesatyy for preliminary MS/MS experiments and valuable discussions about tandem mass spectrometry techniques and detection of post-translational modifications, and the Funcional Genomics Center Zurich (fgcz) for measuring our samples and providing us with appropriate and up-to-date software for data evaluation. Thanks go also to Teresa Colangelo Failla for help with the 2D gel electrophoresis. Åsa Frederiksson and Thomas Nyström generously supported us with their experience and knowledge while establishing the Oxyblot method in our laboratory.

#### References

- Ackermann, M., Stearns, S.C., and Jenal, U. (2003) Senescence in a bacterium with asymmetric division. *Science* **300**: 1920.
- Ballesteros, M., Fredriksson, A., Henriksson, J., and Nyström, T. (2001) Bacterial senescence: protein oxidation in non-proliferating cells is dictated by the accuracy of the ribosomes. *EMBO J* **20**: 5280-5289.
- Berlett, B.S., and Stadtman, E.R. (1997) Protein oxidation in aging, disease, and oxidative stress. *J Biol Chem* **272**: 20313-20316.
- Berney, M., Weilenmann, H.-U., and Egli, T. (2006) Flow-cytometric study of vital cellular functions in *Escherichia coli* during solar disinfection (SODIS). *Microbiology* **152**: 1719-1729.
- Berney, M., Weilenmann, H.-U., and Egli, T. (2007) Adaptation to UVA radiation of *E. coli* growing in continuous culture. *J Photochem Photobiol B* **86**: 149-159.
- Bosshard, F., Bucheli, M., Meur, Y., and Egli, T. (2009a) The respiratory chain is the cells Achilles' heel during UVA inactivation in *Escherichia coli*. *Microbiology* (in press): doi: 10.1099/mic.0.038471-0
- Bosshard, F., Berney, M., Scheifele, M., Weilenmann, H.-U., and Egli, T. (2009b) Solar disinfection (SODIS) and subsequent dark storage of *Salmonella typhimurium* and *Shigella flexneri* monitored by flow cytometry. *Microbiology* **155**: 1310-1317.

- Bourdon, E., and Blache, D. (2001) The importance of proteins in defence against oxidation. *Antioxid Redox Signal* **3**: 293–311.
- Bradford, M.M. (1976) A rapid and sensitive method for the quantitation of microgram quantities of protein utilizing the principle of protein-dye binding. *Anal Biochem* **72**: 248–254.
- Cabiscol, E., Tamarit, J., and Ros, J. (2000) Oxidative stress in bacteria and protein damage by reactive oxygen species. *Int Microbiol* **3**: 3–8.
- Chiti, F. (2006) Relative importance of hydrophobicity, net charge and secondary structure propensities in protein aggregation. In *Protein Misfolding, Aggregation and Conformational Diseases; Part A: Protein Aggregation and Conformational Diseases*. Uversky, V.N., and Fink, A.L. (eds). Berlin, Germany: Springer, pp. 43–59.
- Choksi, K.B., Nuss, J.E., DeFord, J.H., and Papaconstantinou, J. (2008) Age-related alterations in oxidatively damaged proteins of mouse skeletal muscle mitochondrial electron transport chain complexes. *Free Radic Biol Med* **45**: 826–838.
- Conroy, R.M., Meegan, M.E., Joyce, T., McGuigan, K., and Barnes, J. (2001) Solar disinfection of drinking water protects against cholera in children under 6 years of age. *Arch Dis Child* **85**: 293–295.
- Daly, M.J., Gaidamakova, E.K., Matrosova, V.Y., Vasilenko, A., Zhai, M., Leapman, R.D., et al. (2007) Protein oxidation implicated as the primary determinant of bacterial radioreistance. *PLoS Biol* **5**: 769–779.
- Davies, K.J. (1987) Protein damage and degradation by oxygen radicals. I. General aspects. *J Biol Chem* **262**: 9895–9901.
- Davies, K.J., and Delsignore, M.E. (1987) Protein damage and degradation by oxygen radicals. III. Modification of secondary and tertiary structure. *J Biol Chem* **262**: 9908–9913.
- Davies, K.J., and Lin, S.W. (1988) Oxidatively denatured proteins are degraded by an ATP-independent proteolytic pathway in *Escherichia coli*. *Free Radic Biol Med* **5**: 225–236.
- Desnues, B., Cuny, C., Dukan, S., Grégori, G., Aguilaniu, H., and Nyström, T. (2003) Differential oxidative damage and expression of stress defence regulons in culturable and non-culturable *Escherichia coli* cells. *EMBO Rep* **4**: 400–404.
- Dukan, S., and Nystrom, T. (1998) Bacterial senescence: stasis results in increased and differential oxidation of cytoplasmic proteins leading to developmental induction of the heat shock regulon. *Genes Dev* **12**: 3431–3441.
- Dukan, S., and Nystrom, T. (1999) Oxidative stress defence and deterioration of growth-arrested *Escherichia coli* cells. *J Biol Chem* **274**: 26027–26032.
- Franchini, A.G. (2006) Physiology and fitness of *Escherichia coli* during growth in carbon-excess and carbon-limited environments. ETH PhD Thesis No. 16585. Zurich, Switzerland.
- Fredrickson, J.K., Li, S.M.W., Gaidamakova, E.K., Matrosova, V.Y., Zhai, M., Sulloway, H.M., et al. (2008) Protein oxidation: key to bacterial desiccation resistance? *ISME J* **2**: 393–403.
- Friguet, B. (2006) Oxidized protein degradation and repair in aging and oxidative stress. *FEBS Lett* **580**: 2910–2916.
- Gallagher, S.R. (2006) One-dimensional SDS gel electrophoresis of proteins. *Curr Prot Immunol Unit* **8.4**.
- Gardner, P.R., and Fridovich, I. (1991) Superoxide sensitivity of the *Escherichia coli* aconitase. *J Biol Chem* **266**: 19328–19333.
- Gianazza, E., Crawford, J., and Miller, I. (2007) Detecting oxidative post-translational modifications in proteins. *Amino Acids* **33**: 51–56.
- Grant, R.A., Filman, D.J., Finkel, S.E., Kolter, R., and Hogle, J.M. (1998) The crystal structure of Dps, a ferritin homolog that binds and protects DNA. *Nat Struct Biol* **5**: 294–303.
- Gross, L. (2007) Paradox resolved? The strange case of the radiation-resistant bacteria. *PLoS Biol* **5**: e108.
- Grune, T., Jung, T., Merker, K., and Davies, K.J. (2004) Decreased proteolysis caused by protein aggregates, inclusion bodies, plaques, lipofuscin, ceroid, and 'aggregosomes' during oxidative stress, aging, and disease. *Int J Biochem Cell Biol* **36**: 2519–2530.
- Hoerter, J.D., Arnold, A.A., Ward, C.S., Sauer, M., Johnson, S., Fleming, T., and Eisenstark, A. (2005a) Reduced hydroperoxidase (HPI and HPII) activity in the Deltafur mutant contributes to increased sensitivity to UVA radiation in *Escherichia coli*. *J Photochem Photobiol B* **79**: 151–157.
- Hoerter, J.D., Arnold, A.A., Kuczynska, D.A., Shibuya, A., Ward, C.S., Sauer, M.G., et al. (2005b) Effects of sublethal UVA irradiation on activity levels of oxidative defence enzymes and protein oxidation in *Escherichia coli*. *J Photochem Photobiol B* **81**: 171–180.
- Jakob, U., Muse, W., Eser, M., and Bardwell, J.C. (1999) Chaperone activity with a redox switch. *Cell* **96**: 341–352.
- Jakob, U., Eser, M., and Bardwell, J.C. (2000) Redox switch of hsp33 has a novel zinc-binding motif. *J Biol Chem* **275**: 38302–38310.
- Jeffrey, W.H., Kase, J.P., and Wilhelm, S.W. (2005) UV radiation effects on heterotrophic bacterioplankton and viruses in marine ecosystems. In *The Effects of UV Radiation in the Marine Environment*. De Mora, S., Demers, S., and Vernet, M. (eds). Cambridge, UK: Cambridge University Press, pp. 206–236.
- Keller, A., Nesvizhskii, A.I., Kolker, E., and Aebersold, R. (2002) Empirical statistical model to estimate the accuracy of peptide identifications made by MS/MS and database search. *Anal Chem* **74**: 5383–5392.
- Laemmli, U.K. (1970) Cleavage of structural proteins during the assembly of the head of bacteriophage T4. *Nature* **227**: 680–685.
- Levine, R.L. (2002) Carbonyl modified proteins in cellular regulation, aging, and disease. *Free Radic Biol Med* **32**: 790–796.
- Levine, R.L., and Stadtman, E.R. (2001) Oxidative modification of proteins during aging. *Exp Gerontol* **36**: 1495–1502.
- Lindner, A.B., Madden, R., Dernarez, A., Stewart, E.J., and Taddei, F. (2008) Asymmetric segregation of protein aggregates is associated with cellular aging and rejuvenation. *Proc Natl Acad Sci USA* **105**: 3076–3081.
- Long, J., Liu, C., Sun, L., Gao, H., and Liu, J. (2009) Neuronal mitochondrial toxicity of malondialdehyde: inhibitory effects on respiratory function and enzyme activities in rat brain mitochondria. *Neurochem Res* **34**: 786–794.

- Lund, M.N., Luxford, C., Skibsted, L.H., and Davies, M.J. (2008) Oxidation of myosin by haem proteins generates myosin radicals and protein cross-links. *Biochem J* **410**: 565–574.
- Maisonneuve, E., Ezraty, B., and Dukan, S. (2008a) Protein aggregates: an aging factor involved in cell death. *J Bacteriol* **190**: 6070–6075.
- Maisonneuve, E., Fraysse, L., Lignon, S., Capron, L., and Dukan, S. (2008b) Carbonylated proteins are detectable only in a degradation-resistant aggregate state in *Escherichia coli*. *J Bacteriol* **190**: 6609–6614.
- Maisonneuve, E., Fraysse, L., Moinier, D., and Dukan, S. (2008c) Existence of abnormal protein aggregates in healthy *Escherichia coli* cells. *J Bacteriol* **190**: 887–893.
- Mazzulli, J.R., Hodara, R., Lind, S., and Ischiropoulos, H. (2006) Oxidative stress and protein deposition diseases. In *Protein Misfolding, Aggregation and Conformational Diseases; Part A: Protein Aggregation and Conformational Diseases*. Uversky, V.N., and Fink, A.L. (eds). Berlin, Germany: Springer, pp. 123–133.
- Mirzaei, H., and Regnier, F. (2005) Affinity chromatographic selection of carbonylated proteins followed by identification of oxidation sites using tandem mass spectrometry. *Anal Chem* **77**: 2386–2392.
- Mirzaei, H., and Regnier, F. (2006a) Creation of allotypic active sites during oxidative stress. *J Proteome Res* **5**: 2159–2168.
- Mirzaei, H., and Regnier, F. (2006b) Protein-RNA cross-linking in the ribosomes of yeast under oxidative stress. *J Proteome Res* **5**: 3249–3259.
- Mirzaei, H., and Regnier, F. (2007) Identification of yeast oxidized proteins: chromatographic top-down approach for identification of carbonylated, fragmented and cross-linked proteins in yeast. *J Chromatogr A* **1141**: 22–31.
- Neidhardt, F.C., Ingraham, J.L., and Schaechter, M. (1990) *Physiology of the Bacterial Cell: A Molecular Approach*. Sunderland, MA, USA: Sinauer Associates.
- Nesvizhskii, A.I., Keller, A., Kolker, E., and Aebersold, R. (2003) A statistical model for identifying proteins by tandem mass spectrometry. *Anal Chem* **75**: 4646–4658.
- Nyström, T. (2003) Nonculturable bacteria: programmed survival forms or cells at death's door? *Bioessays* **25**: 204–211.
- Nyström, T. (2005) Role of oxidative carbonylation in protein quality control and senescence. *EMBO J* **24**: 1311–1317.
- Nyström, T. (2006) Oxidative damage and cellular senescence: lessons from bacteria and yeast. In *Redox Proteomics: From Protein Modifications to Cellular Dysfunction and Diseases*. Dalle-Donne, I., Scaloni, A., and Butterfield, D.A. (eds). New Jersey, USA: John Wiley & Sons, pp. 473–484.
- Nyström, T. (2007) A bacterial kind of aging. *PLoS Genet* **3**: e224.
- Requena, J.R., Levine, R.L., and Stadtman, E.R. (2003) Recent advances in the analysis of oxidized proteins. *Amino Acids* **25**: 221–226.
- Shacter, E., Williams, J.A., Lim, M., and Levine, R.L. (1994) Differential susceptibility of plasma proteins to oxidative modification: examination by western blot immunoassay. *Free Radic Biol Med* **17**: 429–437.
- Shevchenko, A., Wilm, M., Vorm, O., and Mann, M. (1996) Mass spectrometric sequencing of proteins silver-stained polyacrylamide gels. *Anal Chem* **68**: 850–858.
- Squier, T.C. (2001) Oxidative stress and protein aggregation during biological aging. *Exp Gerontol* **36**: 1539–1550.
- Stadtman, E.R. (2006) Protein oxidation and aging. *Free Radic Res* **40**: 1250–1258.
- Stadtman, E.R., and Levine, R.L. (2003) Free radical-mediated oxidation of free amino acids and amino acid residues in proteins. *Amino Acids* **25**: 207–218.
- Stewart, E.J., Madden, R., Paul, G., and Taddei, F. (2005) Aging and death in an organism that reproduces by morphologically symmetric division. *PLoS Biol* **3**: e45.
- Tamarit, J., Cabisco, E., and Ros, J. (1998) Identification of the major oxidatively damaged proteins in *Escherichia coli* cells exposed to oxidative stress. *J Biol Chem* **273**: 3027–3032.
- Terman, A., and Brunk, U.T. (2006) Oxidative stress, accumulation of biological 'garbage', and aging. *Antioxid Redox Signal* **8**: 197–204.
- Varghese, S., Tang, Y., and Imlay, J.A. (2003) Contrasting sensitivities of *Escherichia coli* aconitases A and B to oxidation and iron depletion. *J Bacteriol* **185**: 221–230.
- Voss, P., Hajimiragha, H., Engels, M., Ruhwiedel, C., Calles, C., Schroeder, P., and Grune, T. (2007) Irradiation of GAPDH: a model for environmentally induced protein damage. *Biol Chem* **388**: 583–592.
- Wegelin, M., Canonica, S., Mechsner, K., Fleischmann, T., Pesaro, F., and Metzler, A. (1994) Solar water disinfection: scope of the process and analysis of radiation experiments. *J Water SRT – Aqua* **43**: 154.
- Wickner, S., Maurizi, M.R., and Gottesman, S. (1999) Post-translational quality control: folding, refolding, and degrading proteins. *Science* **286**: 1888–1893.
- Winter, J., Linke, K., Jatzek, A., and Jakob, U. (2005) Severe oxidative stress causes inactivation of DnaK and activation of the redox-regulated chaperone Hsp33. *Mol Cell* **17**: 381–392.
- Yuanbin, L., Gary, F., and David, S. (2002) Generation of reactive oxygen species by the mitochondrial electron transport chain. *J Neurochem* **80**: 780–787.